

# Measurement of fluidised bed dryer by different frequency and different normalisation methods with electrical capacitance tomography

H G Wang and W Q Yang

School of Electrical and Electronic Engineering, The University of Manchester, Manchester, UK,  
[haigang.wang@manchester.ac.uk](mailto:haigang.wang@manchester.ac.uk)

## Abstract

An electrical capacitance tomography (ECT) sensor has been mounted near the bottom of a fluidised bed dryer. An ECT system based on an HP4128 impedance analyser has been used to measure capacitance and loss conductance between the electrode pairs in the sensor. It has been found that the capacitance depends on not only the particle moisture but also the frequency. With low moisture content, the relationship between capacitance and frequency is simple and linear. With high moisture content, however, the relationship becomes more complex and non-linear. For image reconstruction, different normalisation models have been used: series, parallel and Maxwell. The results show that with low moisture content, the three models give nearly the same image error. With the increase in moisture content, the difference between the three models becomes more and more obvious. With different gas-solids flow patterns, the three models also give slightly different images.

**Keywords:** Fluidised bed dryer, Particle moisture, Spectroscopy, Normalisation model, Electrical capacitance tomography

## Introduction

Fluidised bed dryers have been widely used in the pharmaceutical, food, chemical process and other industries for many years (Vojtěch *et al.* 1966). To investigate the solids distribution during a drying process, electrical capacitance tomography (ECT) has been applied to a lab-scale fluidised bed dryer (Chaplin *et al.* 2005a, 2005b, Wang *et al.* 2008). While some advantages of using ECT to investigate fluidisation processes over the conventional methods (Makkawi and Wright 2004, Liu *et al.* 2002), the application of ECT in fluidised bed dryers has encountered some difficulties because of the moisture content changes during the drying process (McKeen and Pugsley 2002, Wang *et al.* 2008). Typically, during a drying process, the moisture content of granule changes from say 30% to 1%, which results in the change in the dielectric properties of material (Robinson *et al.* 1999, Sacilik *et al.* 2006), including permittivity, dielectric loss and conductivity. The changes in permittivity and conductivity results in the change in measured capacitance and conductance. In the past, the frequency is normally kept constant and also in the low frequency range, typically between 100 kHz and 200 kHz (Chaplin *et al.* 2005a, 2005b, Wang *et al.* 2008). With a fixed low frequency, good results can be obtained when the moisture content is lower than a certain level, say 18% (Wang *et al.* 2008). With a high moisture content, however, images are reconstructed less accurately and sometimes a wrong solids distribution may be given.

As well known, the dielectric properties of many materials are frequency-dependent and a function of material moisture and density (Mamishv *et al.* 2002, Kraszewski and Nelson 1989). To improve the measurement accuracy, it is necessary to use an ECT system with a suitable frequency.

The ultimate objectives of this research are to provide accurate measurement of fluidised bed drying and to control a fluidised bed dryer effectively for improved operation efficiency.

## Dielectric properties and normalisation methods

The dielectric properties to be considered include permittivity and loss factor. The permittivity  $\varepsilon'$  referred to a free space is the capacitance of a unit volume of matter divided by the permittivity of free space. The loss factor  $\varepsilon''$  can be defined as the conductance of a unit volume of matter divided by  $\omega\varepsilon_0$ . The complex permittivity and the loss tangent of the material are

$$\varepsilon = \varepsilon' - j\varepsilon'' \quad (1)$$

$$\tan \delta = \varepsilon'' / \varepsilon' \quad (2)$$

Where  $\delta$  is the loss angle of the dielectric material.

The dielectric properties of wet bulk granule depend upon the density and moisture content of the material as well as the frequency. The effects of moisture content and frequency on capacitance and loss conductance are considered. In general, the dielectric properties of granule are known to be dependent on moisture content, bulk density, temperature and frequency (Sacilik *et al.* 2006, Mamishev *et al.* 2002). In this study the dielectric properties of static samples are measured at different frequency in the range of 50 kHz-13 MHz with moisture content in the range of 1.5-38%. The effect of bulk density of solids on the dielectric properties is neglected in this research. Some details about the effect of bulk density can be read in (Kraszewski and Nelson 1989, Brosseau and Beroual 2001, Mamishev *et al.* 2002).

In this research, three normalisation models are used: series, parallel and Maxwell, which are given by

$$C_{NS} = \frac{C_M - C_L}{C_H - C_L} \quad (3)$$

$$C_{NP} = \frac{\frac{1}{C_M} - \frac{1}{C_L}}{\frac{1}{C_M} - \frac{1}{C_H}} \quad (4)$$

$$C_{NM} = \frac{C_{NS} \cdot (2.0 + k)}{(3.0 + C_{NS}) \cdot (k - 1.0)} \quad (5)$$

In equation (5),  $k$  is the ratio of high and low permittivity values,  $C_M$  is the measured capacitance,  $C_L$  is the capacitance when the ECT sensor is empty and  $C_H$  is the capacitance when the sensor is filled with wet granule.

The high permittivity is for wet granule and the low permittivity is for hot air. The relationship between the measured capacitance and the normalised capacitance for different distribution was presented in a previous paper (Yang *et al.* 1999). They are used to evaluate the effects of frequency on image reconstruction for different solids distributions with different moisture content.

The Landweber iteration has been used to reconstruct solids distribution (Yang *et al.* 1999, 2002). Because of the non-linear problems, a relaxation factor is often employed to ensure convergence to seek an iterative solution to strongly nonlinear equations (Patankar 1980, Yang and Peng 2003). A relaxation factor is used in the Landweber iteration algorithm to avoid divergence and the algorithm is written as

$$G^{n+1} = G^n \cdot (1.0 + \omega) + \alpha \cdot S^T \cdot (C_N - S \cdot G^n) \cdot (1 - \omega) \quad (6)$$

Where  $\alpha$  is the step length or gain factor and  $\omega$  is the relaxation factor.

An optimum method can be used to choose the step length (Liu *et al.* 1999). However, there are no general rules for choosing the best value for the relaxation factor. The optimum value depends upon a number of factors, e.g. the nature of the problem, the number of grid points, the grid spacing, and the iteration procedure used (Patankar 1980). When  $\omega$  is set to be zero, the iteration becomes the conventional Landweber iteration. If it is negative, the iteration is called under-relaxation. If it is positive it is called over-relaxation (Patankar 1980). In this research, the value is decided by tried-and-error.

### Experiment method

It is well known that the gas-solids behaviour in fluidised beds is more complicated than other gas-solids process, e.g. pneumatic conveying and spouted beds (Davidson *et al.* 1985, Kunii and Levenspiel 1991). To verify the above assumption, an ECT sensor has been mounted near the bottom of a lab-scale fluidised bed dryer from Sherwood (Tornado M501). An ECT system based on an HP4128 impedance analyser (Yang 2007) has been used to measure capacitance and loss conductance between electrode pairs in the ECT sensor. During experiment, the frequency was changed from 50 kHz to 13 MHz and the moisture content changed from 1.5-38%.

The choice of normalisation model is important for image reconstruction of different distributions (Yang *et al.* 2004). Series, parallel and Maxwell models are used to normalise the measured capacitance. Four typical gas solids distributions, i.e., annular, core, stratified and mixing distributions were tested with the normalisation models and the effects of frequency on imaging reconstruction. To evaluate the image quality, two parameters, namely image error and capacitance residual, were used (Yang and Peng 2003).

A type of wet granule, semolina, is used. The properties of this type of granule can be found in a paper (Erbaş *et al.* 2005). For preparation of the wet granule with different moisture content, water was sprayed onto dry material and mixed in a low-speed food mixer (KENWOOD CHEF) for 10-20 minutes. The granulation product was then sieved through a 1.5 mm screen to remove large particles due to agglomeration of wet fine particles and make sure each batch to start from the same bulk density. The moisture content was measured by an HB43 moisture meter from Mettler-Toledo as reference. The impedance analyser was programmed to measure the dielectric properties of granule at different frequencies in the range from 50 kHz to 13 MHz. Details of the system hardware and operation were given in a PhD thesis (Yang 2007). The ECT sensor has 8 electrodes, with the wall of the fluidised beds dryer as the frame of the sensor, and is enclosed by an earthed screen to eliminate external interface. An opposite electrode pair, 1 and 5, is used to determine the dielectric properties. The permittivity, conductivity and dielectric loss can be deduced from the measured capacitance and conductance.

The experiments were carried out in a laboratory with a room temperature of  $20 \pm 2^\circ\text{C}$ . To reduce the effect of bulk particle density, for each batch measurement, the samples were poured into the glass tube and then fluidised for half minutes by cold air at the minimum fluidisation condition. After switching off the air supply, the sample settles down freely and a natural packing condition can be achieved with almost the same bulk particle voidage fraction of 65%.

### Effects of frequency and moisture content on dielectric property measurements

The variations in capacitance, conductance, dielectric loss and loss tangent with the frequency in the range of 100 kHz-10 MHz for different moisture content are shown in Fig. 1. In the frequency range of 50 kHz-4 MHz, the measured capacitance decreases with an increase in frequency when the moisture content is lower than 20%. With high moisture content, the measured capacitance increases with the increase in frequency. In general, the capacitance with high moisture content is smaller than that with low moisture content when the frequency is lower than 1 MHz. When the frequency is higher than 4 MHz, the capacitance increases with the increase in frequency for all the cases with different moisture content. From Fig. 1 (b), it can be seen that the conductivity increases with the increase in frequency. The difference is that the change becomes faster and faster with the increase in moisture content. The capacitance as shown in Fig. 1 (a) is less regular than the results measured with a parallel plat capacitor (Sacilik *et al.* 2006), because of different geometry.

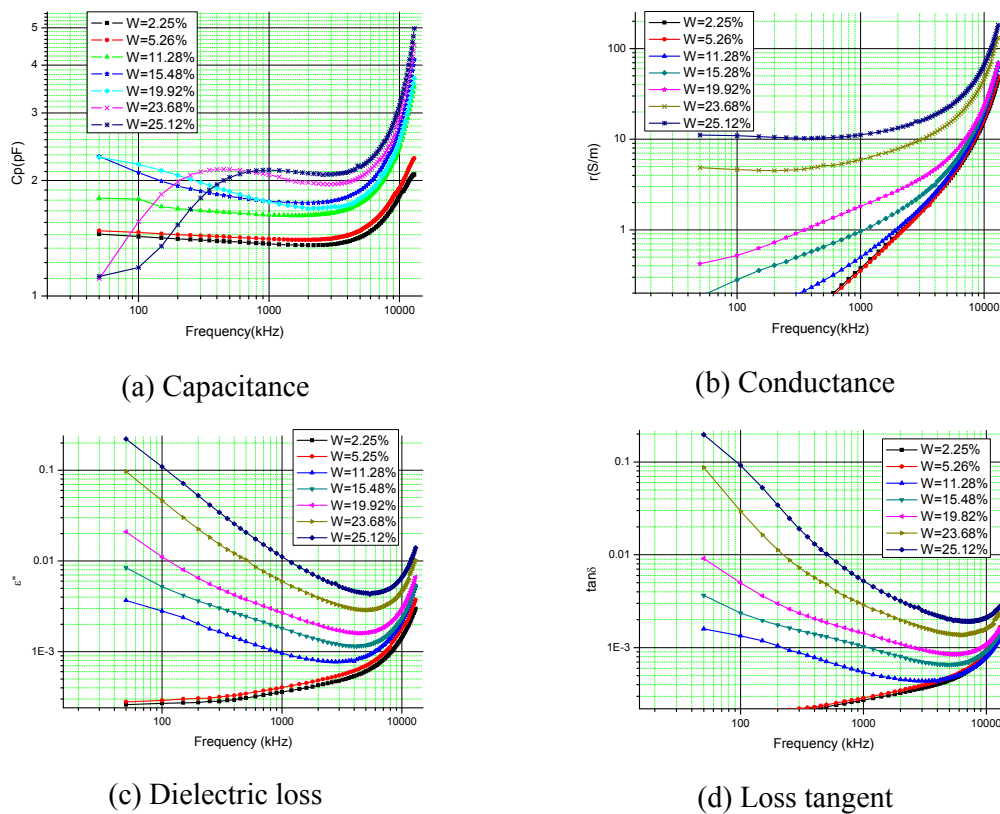
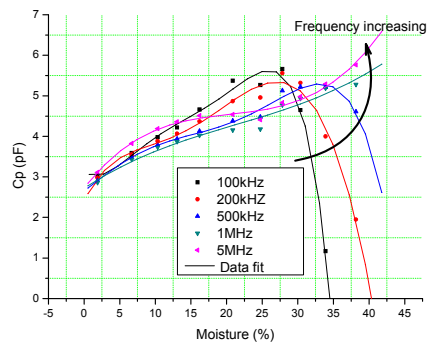


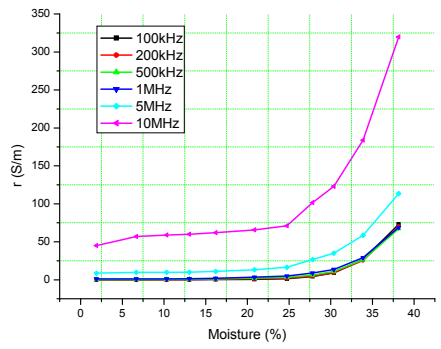
Fig. 1 Variation in dielectric properties with frequency at different moistures

The dielectric loss is shown in Fig. 1 (c). With low moisture content, the loss increases with the increase in frequency. With high moisture content, however, the value first decreases with the increase in frequency and then increases with the increase of frequency. The loss tangent has the same trend as dielectric loss. At a low frequency, e.g. 100 kHz, the dielectric loss for 25.1% water is

more than 100 times bigger than that of 5.1% water. At a high frequency, say 10 MHz, this value is close to each other, with only a few times difference. These characteristics can be clearly seen in Fig. 1 (c).

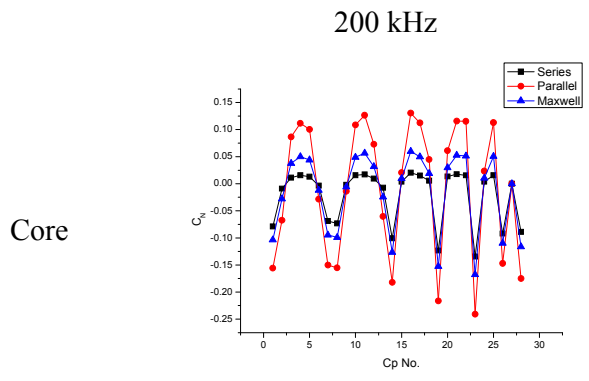


(a) Capacitance

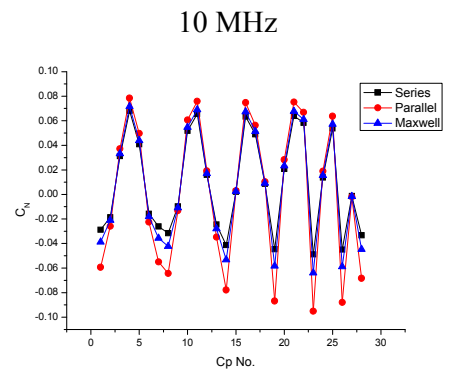


(b) Conductivity

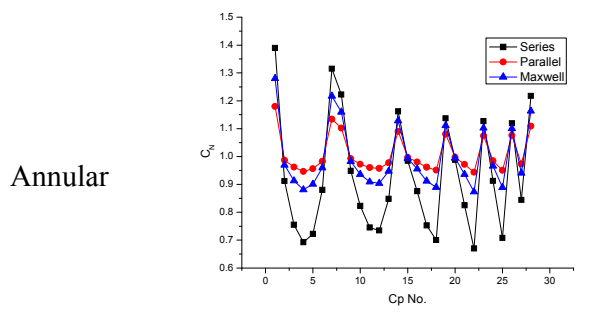
Fig. 2 Variation in capacitance and conductivity with moisture content and frequency



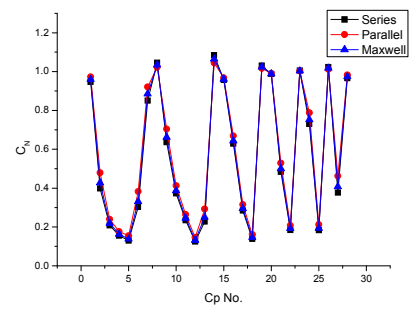
(a)



(b)

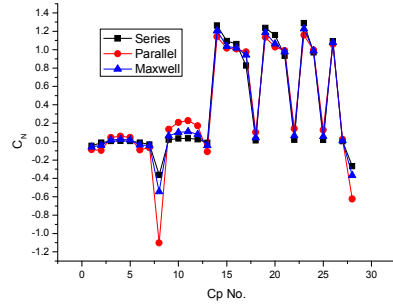


(c)

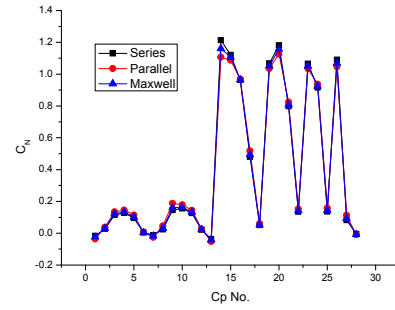


(d)

Stratified



(e)



(f)

Fig. 3 Normalised capacitance

Fig. 2 shows the change in capacitance and conductance with moisture content at different frequency. It is clear that the trend for capacitance is more complex than that for conductance. With the increase in frequency, the relationship between capacitance and moisture changes from non-linear to linear as shown in Fig. 2 (a). With low moisture content, the relationship between capacitance and moisture content is non-linear. With high moisture content, the relationship becomes simple and linear. The change in conductance has the same trend for all the moisture content levels as shown in Fig. 2 (b). All these complex characteristics of dielectric properties are mostly due to the effect of water in such porous material.

From the above results, it can be seen that the moisture content and frequency strongly affect capacitance. In a fluidised bed dryer, in the first drying stage, especially in the beginning of drying process, the moisture content normally is more than 20.0%. In such a condition, the conventional measurement methods of ECT with a fixed frequency may not be suitable. Therefore, it may be necessary to use an ECT system with programmable frequency and with different normalisation models.

### Image reconstruction with different normalisation model

Fig. 3 shows the normalised capacitance with different models for different distribution at two different frequencies. At low frequency, the three models give different normalised values. At high frequency, however, they nearly give the same results. It is clear to see which model is better from the reconstructed images.

Fig. 4 gives the image reconstruction results for three distributions with different normalisation models. For stratified and core distributions, the parallel model gives the best results. For an annular distribution, the series model gives better images than other two models. It seems that the reconstructed images are much better if the span between the minimum and maximum capacitance is bigger. For an annular distribution, this trend is clear with the series model. For core and stratified distributions, the parallel and Maxwell models are better than the series model.

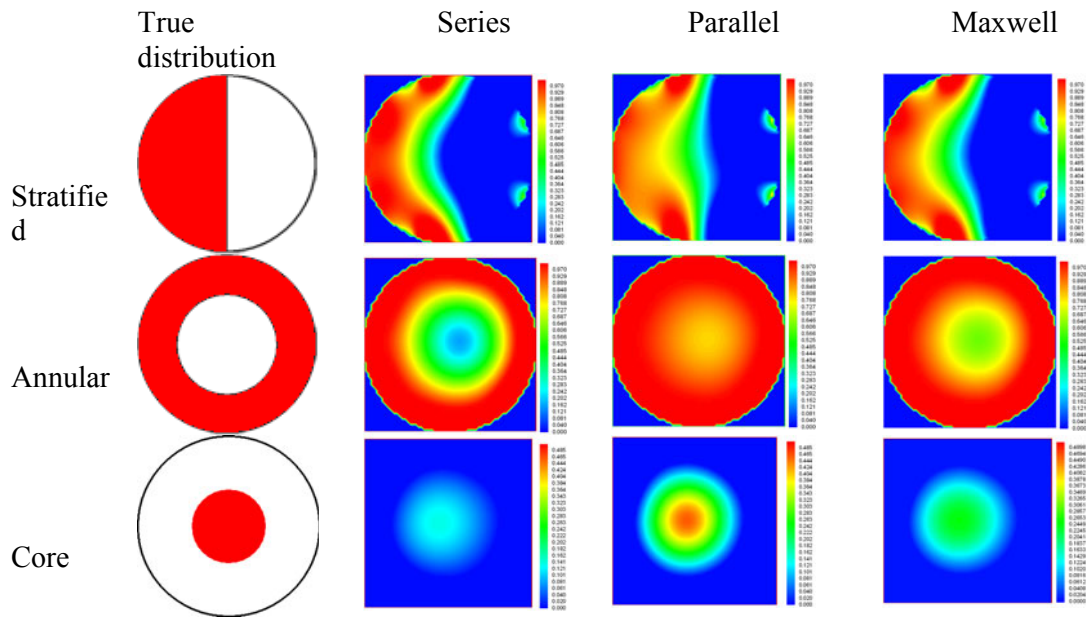
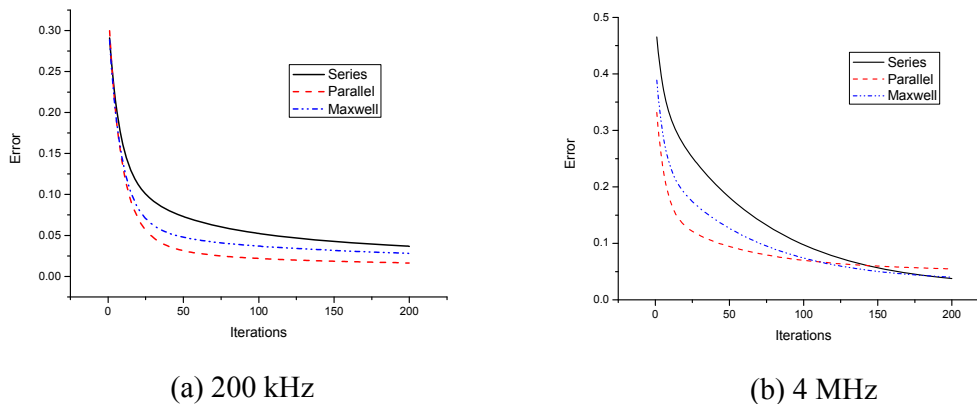


Fig. 4 Reconstructed images for 5.0% water at 200 kHz

To evaluate image quality, two parameters are used: capacitance residual and image error. The definition of these parameters can be found in (Yang and Peng 2003). Fig. 5 gives the capacitance residual for core distributions. At low frequency, the parallel model gives the minimum value and the series model gives the maximum values. At high frequency, in the end of iteration, these three models give similar results.



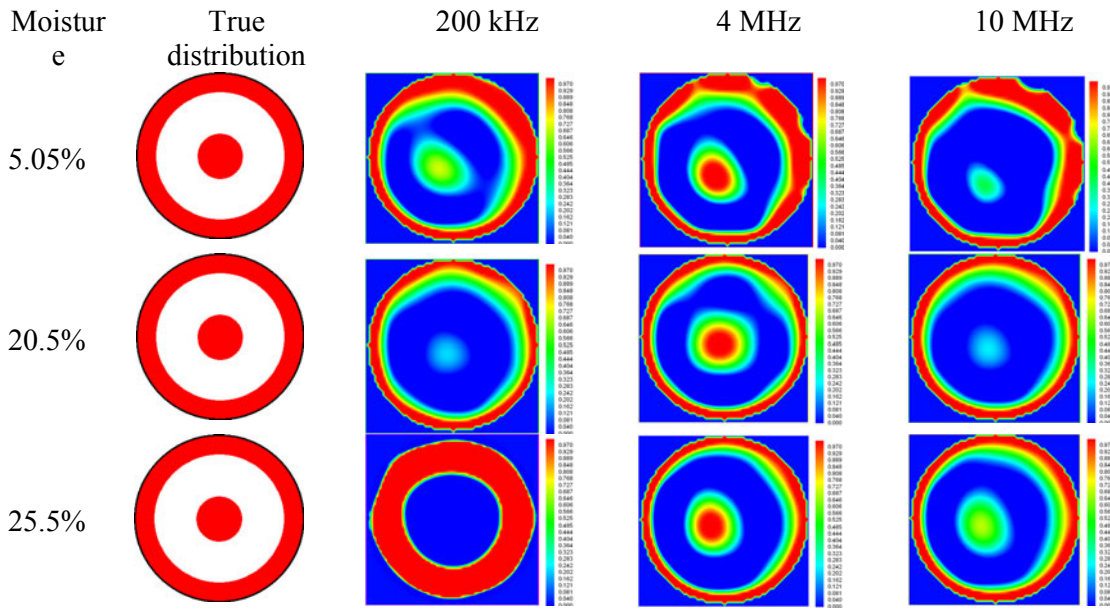
(a) 200 kHz

(b) 4 MHz

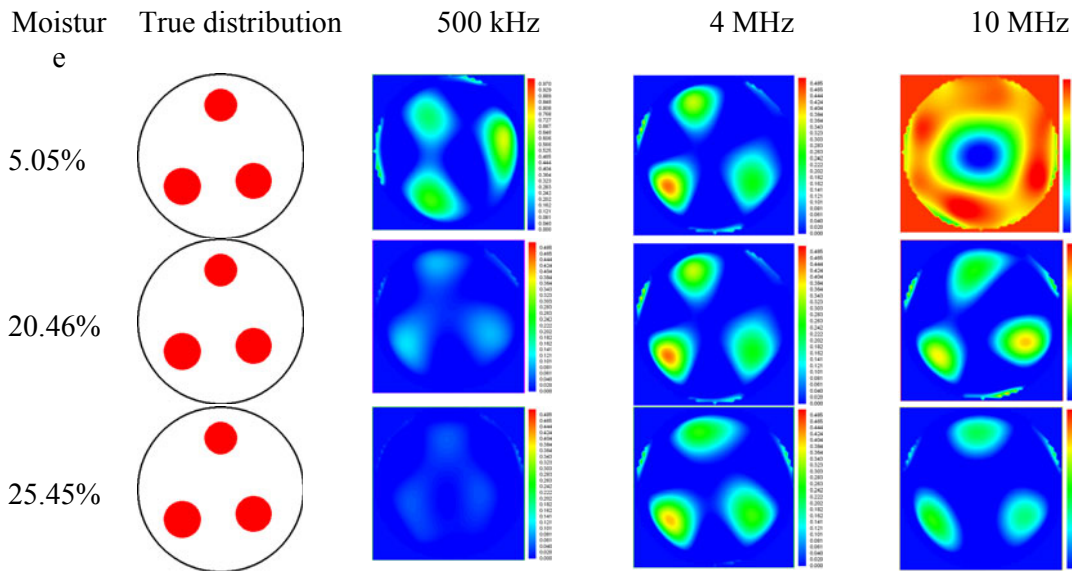
Fig. 5 Capacitance residual with different normalised models and frequency for core distribution

Figs. 6 shows the effect of frequency and moisture content on image reconstruction with different normalisation models. Fig. 6 (a) gives the result for annular-core distributions and Fig. 6 (b) shows three robs distribution. For these two types of distributions, the best results are obtained for all the moisture content with 4 MHz. At low frequency, only with low moisture content, image reconstruction is good. Fig. 7 gives the capacitance residual for three rob distribution at different frequency. Fig. 8 gives the image error for this type of distribution. From the capacitance residual results, it can be seen that high frequency gives a low capacitance residual. From Fig. 8, it can be seen that with a relaxation factor, the iteration process becomes more stable and trends to converge.

Also it can be seen that for the three rob distribution, the parallel and Maxwell models gives more accurate results than the series model. All these results are summarised in Tables 1 to 3.



(a) Annul-core distribution

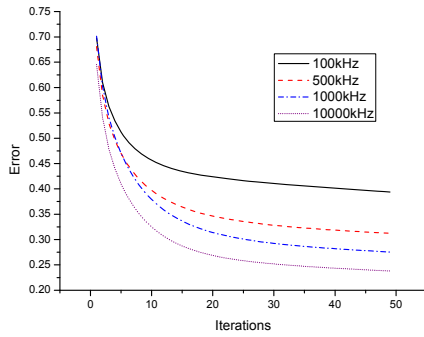


(b) Three robs distribution

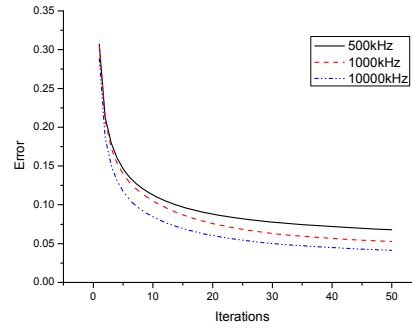
Fig. 6 Image reconstruction of annul-core and three robs distributions

From Tables 1 and 2, it can be seen that for different moisture contents, 500 kHz frequency always gives slightly bigger image error than 1 or 4 MHz. With the increase in frequency, the image error becomes smaller and smaller. However, with the further increase in frequency, the image error increases again, because the stray capacitance of ECT sensor increases with the increase in frequency (Yang 2007). It can also be seen from Tables 1 and 2 that the Maxwell model gives the best results compared with the series and parallel models for these two complex distributions.





(a)  $W = 5.67\%$

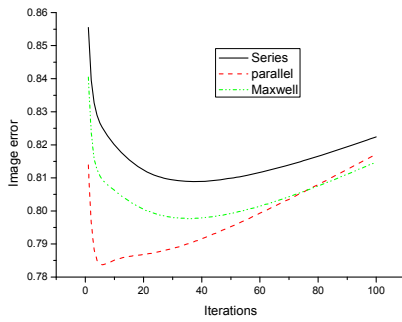


(b)  $W = 29.7\%$

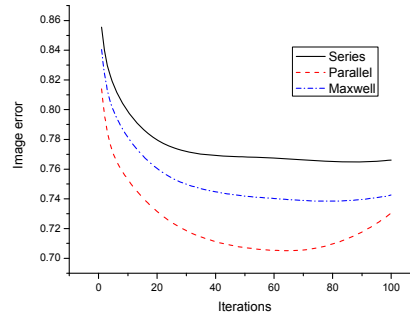
Fig. 7 Error with different frequency vs. iteration for core distribution

Table 1 Image error for annular-core distribution

	$W = 5.05\%$			$W = 24.7\%$		
	Series	Parallel	Maxwell	Series	Parallel	Maxwell
500 kHz	79.1	68.7	65.2	98.3	59.6	51.1
1 MHz	56.6	61.0	62.5	45.2	51.1	45.2
10 MHz	70.2	72.0	72.6	56.9	60.5	61.7



(a) Conventional Landweber



(B) Landweber with relaxation factor

Fig. 8 Image error with different normalisation models

Table 2 Image error for three robs distribution

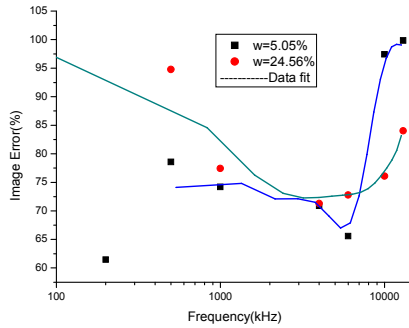
	$W = 5.05\%$			$W = 24.7\%$		
	Series	Parallel	Maxwell	Series	Parallel	Maxwell
500 kHz	85.0	79.4	78.6	94.5	96.0	94.8
4 MHz	72.0	71.2	70.9	75.9	72.6	71.3
10 MHz	97.4	97.4	97.4	78.8	76.9	76.1

Table 3 shows the results of capacitance residual for annular-core distributions. For different moisture contents, low frequency always gives the biggest capacitance error. With the increase in frequency, the error tends close to zero. Note that small capacitance error does not necessarily mean good image (Yang and Peng 2003). This can be seen clearly from the image error as listed in Table 1.

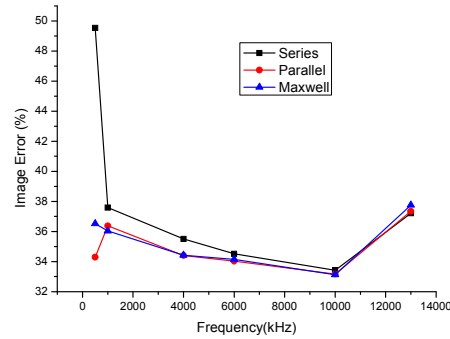
Fig. 9 gives the variations in image error with different frequency for different moisture content and normalisation models. This result shows that with low moisture content, the image error nearly keeps the same level in the low frequency range. For high moisture content, the image error is lower in the middle frequency range and high in both low and high frequency ranges. With the same moisture content, in the low frequency range, the result with the series model is worse than the parallel and Maxwell models. At high frequency, these three models give nearly the same image errors. From these results, it can be seen that the choice of a normalisation model play an importance role in imaging reconstruction in the low frequency rang.

Table 3 Capacitance residual for annular-core distribution

	W = 5.15%	W = 20.7%	W = 24.7%
200 kHz	7.15	11.7	21.0
500 kHz	2.46	2.13	18.7
1 MHz	2.75	2.85	12
4 MHz	2.45	2.18	3.02
6 MHz	2.16	2.12	2.32
10 MHz	2.60	2.22	2.18



(a) Three robs distribution



(b) Core distribution

Fig. 9 Image error vs. frequency

### Conclusions

An ECT system based on an HP 4128 impedance analyser has been used to measure capacitance from a multi-electrode sensor mounted near the bottom of a fluidised bed dryer, showing that capacitance, loss factor, loss tangent, and conductance are functions of the moisture content and frequency. The change in capacitance is dominated by moisture content. The change in capacitance with frequency is higher with larger moisture content. The loss factor and loss tangent depend on frequency more regularly than capacitance. The conductance increases more rapidly with the increase in frequency than the increase in moisture content.

For stratified and core distributions, the parallel model gives better results than the series and Maxwell models. For an annular distribution, the series model gives the best result. For a complex distribution, e.g. annular-core and multi objects distributions, the Maxwell model gives the best images than other two normalisation models. However, the difference between these three models is only obvious when the frequency is lower than 1 MHz. With the increase in frequency, they nearly give the same results.

In fluidised bed dryers, the solids distribution is complex and dynamic. It is useful to combine these three normalisation models together to image the solids distribution. Also, the frequency should be considered when ECT is used to measure a drying process, especially in the warming-up and constant drying periods due to high moisture content.

### Acknowledges

The authors would like to thank EPSRC (GR/T29383/01, GR/T29376/01, EP/G005702/1) and the University of Manchester Intellectual Property (UMIP) Ltd for financially supporting this research. Peter Senior and Rambali Sundara Raghavan from School of Chemical Engineering and analytical Science are thanked for working on a joint project. Oxford University, GEA Process Engineering Ltd, Sherwood Scientific Ltd, DuPont, AstraZeneca and Sensatech Research Ltd are also thanked for their collaboration.

### References

1. Brosseau C and Beroual A (2001), Effective permittivity of composites with stratified particles, *Journal of Physics D: Applied Physics*, 34, pp 704-710
2. Chaplin G, Pugsley T, van der Lee L, Kantzas A and Winters C (2005), The dynamic calibration of an electrical capacitance tomography sensor applied to the fluidized bed drying of pharmaceutical granule, *Meas. Sci. Technol.*, 16, pp 1281-1290
3. Chaplin G and Pugsley T (2005), application of electrical capacitance tomography to the fluidized bed drying of pharmaceutical granule, *Chemical Engineering Science*, 60, pp 7022-7033
4. Davidson J F, Clift R and Harrison D (1985), Fluidization, Academic Press, London, UK, pp 331
5. Erbas M, Ertugay M F and Certel M (2005), Moisture adsorption behavior of semolina and farina, *Journal of Food Engineering*, 69, pp 191-198
6. Kraszewski A and Nelson S O (1989), Composite Model of the complex permittivity of cereal grain, *J. Agric. Engng Res.*, 43, pp 211-219
7. Kunii D and Levenspiel O (1991), Fluidization Engineering, Butterworth-Heinemann, Boston
8. Liu S, Wang H G, Jiang F, Yang W Q (2002), A new image reconstruction method for tomographic investigation of fluidized beds, *AIChE J.*, 48, pp 1631-1638
9. Makkawi Y T and Wright P C (2004), Electrical capacitance tomography for conventional fluidized bed measurements—remarks on the measuring technique, *Powder Technology*, 148, pp 142-157
10. Mamishev A V, Takahashi A R, Du Y, Lesieutre B C and Zahn M (2002), Parameter estimation in dielectrometry measurements, *Journal of electrostatics*, 56, pp 465-492
11. McKeen T R and Pugsley T S (2002), The influence of permittivity models on phantom images obtained from electrical capacitance tomography, *Meas. Sci. Technol.*, 13, pp 1822-1830
12. Robinson D A, Gardner C M K and Cooper J D (1999), Measurement of relative permittivity in sandy solids using TDR, capacitance and theta probes: comparison, including the effects of bulk soil electrical conductivity, *Journal of Hydrology*, 223, pp 198-211
13. Sacilik K, Tarimci C and Colak A (2006), Dielectric properties of flaxseeds as affected by moisture content and bulk density in the ratio frequency range, *Biosystems Engineering*, 93, pp 153-160
14. Suhas V. Patankar (1980), Numerical heat transfer and fluid flow, Hemisphere Publishing Corp, Washington, DC, USA, pp 67-68
15. Vojtěch V C Sc, Markvart M and Drbohlav R (1966), Fluidized bed drying, Leonard Hill, London

16. Wang H G, Yang W Q, Senior P, Raghavan R S and Duncan S R (2008), Investigation of batch fluidized bed drying by mathematical modelling, CFD simulation and ECT measurement, *AIChE J.*, 54, pp 427-444
17. Warsito W and Fan L S (2003), ECT imaging of three-phase fluidized bed based on three-phase capacitance model, *Chemical Engineering Science*, 58, pp 823-832
18. Yang M (2007), Development of electrical tomography systems and application for milk flow metering, PhD thesis, The University of Manchester, Manchester, UK
19. Yang W Q, Chondronasios A, Natrass S, Nguyen V T, Betting M, Ismail I and McCann H (2004), Adaptive calibration of a capacitance tomography system for imaging water droplet distribution, *Flow Measurement and Instrumentation*, 15, pp 249-258
20. Yang W Q, Nguyen T, Betting M, Chondronasios A, Okimoto F and McCann H (2002), Imaging wet gas separation process by capacitance tomography, *IS&T/SPIE 14 Symposium; Electronic Imaging*, San Jose, USA, pp 347-358
21. Yang W Q and Peng L H (2003), Image reconstruction algorithms for electrical capacitance tomography, *Meas. Sci. Technol.*, 14, pp R1-R13
22. Yang W Q, Spink D M, York T A and McCann H (1999), An image-reconstruction algorithm based on Landweber's iteration method for electrical-capacitance tomography, *Meas. Sci. Technol.*, 10, pp 1065-1069